Fabrication and soft magnetic properties of rapidly quenched Co-Fe-B-Si-Nb ultra-thin amorphous ribbons

Ansar Masood[1*], Hasan Ahmadian Baghbaderani[1], Valter Ström[2], Plamen Stamenov[3], Paul McCloskey[1], Cian Ó Mathúna[1, 4], and Santosh Kulkarni[1]

[1]Microsystems Centre, Tyndall National Institute, University College Cork, Cork, Ireland.

[2] Materials Science and Engineering Department, KTH-Royal Institute of Technology, Stockholm, Sweden.

[3]School of Physics and CRANN, Trinity College Dublin, Dublin 2, Ireland.

Abstract:

Ultra-thin soft magnetic amorphous ribbons of Co-Fe-B-Si-Nb alloy were synthesised by a single step rapid-quenching approach to acquire advantage of improved material performance and lower costs over commercial amorphous alloys. The amorphous ribbons of approximately 5.5 µm thicknesses were quenched by a single roller melt spinner in a single-step production process and characterised for their structural and magnetic properties. The disordered atomic structure of amorphous ribbons was confirmed by the x-ray diffraction. A surface morphology study revealed the continuity of ultra-thin ribbons without pores over a large scale. The amorphous alloy showed the ultra-soft magnetic properties in the as-quenched state. The observed thickness dependency of the magnetic properties was attributed to the increased surface roughness and possibly due to a lack of densely packed atomic structure resulting from the extremely high cooling rates experienced by ultra-thin ribbons. We propose that in-situ thinning process of amorphous ribbons significantly reduces the basic material cost and eliminates the need for post-processing steps; hence it provides the opportunity for mass production of high-performance soft magnetic amorphous ribbons at relatively lower costs.

Keywords: Amorphous metals, Ultra-thin ribbons, soft-magnetic properties, high-frequency applications

[*] Corresponding author.
E-mail address: ansar.masood@tyndall.ie.

1. INTRODUCTION

A significant advancement in cutting-edge efficient power switches at high-frequencies has enhanced the need for miniaturised magnetic components in the power converter industry [1-3]. A major challenge in the miniaturisation of power circuitry is the size of passive components which occupy a significant volume fraction (~30%) [4]. The large volume of passive components is due to the ferrite based magnetic cores which are widely used due to their high material loss performance and lower costs. Nevertheless, low magnetic flux density (0.3-0.5 T) of ferrites is a key roadblock in miniaturising the passive component technology [1, 4]. The development of high-flux density low-cost soft magnetic materials to replace bulky ferrite based passive components is a significant challenge to attain the miniaturised power switches at high-frequencies [1, 4].

High-flux density (B_s >1.5 T), exceptionally low coercivity (H_c<10 A/m), and high resistivity (>100 μΩ cm) of amorphous ribbons makes them a potential candidate for high switching frequency applications [5]. The amorphous metal ribbons are typically produced by a rapid-quenching technique and commercially available in the range of 20-30 μm thickness [6-8]. It is widely known that as the operating frequency (f) increases, the eddy-current loss ($W_e \alpha f^2$) increases more sharply than the hysteresis loss ($W_h \alpha f$) and the total core loss dominates by W_e at f > 100 kHz [1, 4]. Eddy currents not only deteriorate the overall magnetic properties but also generate tremendous heat energy, which complicates the design and engineering of the device [1, 6]. The eddy current losses can be significantly reduced by either eliminating the electrically conducting path by using ultra-thin insulated stacks or significantly increase the electrical resistivity of the magnetic material [4]. To get an advantage of eliminated eddy current loss at high frequencies, the thickness of the magnetic material must be smaller than the skin depth δ ($= \sqrt{\frac{\rho}{\pi f \mu}}$, where ρ is resistivity and μ is the permeability) [1, 4]. Thus, to use amorphous metals at MHz frequencies, the thickness of the commercially available amorphous ribbons restricts the use of these novel alloys and hence limits the flux concentration advantage for the miniaturisation of passive components [1, 4].

Recently, we demonstrated a post-processing approach to thin the commercial ribbons to 4 μm by a wet etching route to realise the advantages of material loss performance of soft magnetic amorphous metals at high-frequencies [1, 4]. Nevertheless, wet etching of amorphous metals could be an expensive route at a mass level production as 75% of the material was wasted to reach the required material thickness [1, 4]. Furthermore, the post-processing steps significantly increase the overall cost of the material, hence limits the use of chemically etched ultra-thin ribbons for higher frequency applications. In addition to the amorphous ribbons thickness, the high materials cost of amorphous alloys, due to its high-purity constituent elements, is another challenge to replace the best-in-class ferrites [5, 7, 9]. Interestingly, the use of low-grade industrial materials has been demonstrated to significantly reduce the cost of amorphous metals without deteriorating soft magnetic properties [10]. Further reductions in the cost of amorphous metals, in addition to low-grade industrial compounds, by developing novel approaches of in-situ thinning could be advantageous to replace the ferrites with amorphous metal cores for high-frequency power conversion.

In this work, we demonstrate the rapid quenching approach of in-situ thinning to produce ultra-thin soft magnetic amorphous ribbons. The single step in-situ thinning process of amorphous ribbons provides the opportunity to produce high-performance soft magnetic amorphous ribbons at mass production at lower costs.

2. FABRICATION

Melt-spinning is a well-known technique for making amorphous ribbons. This method uses the molten material to flow from the nozzle in the form of a jet, which comes in contact with rotating copper wheel and procedures a melted puddle. Because of the low viscosity of the molten alloy, the shear layers extend only a few microns from the surface of the roller into the puddle, and it stays on the roller surface. The main advantages of melt-spinning are as follows; (a) production of amorphous ribbons of uniform thickness and width, (2) controlled process parameters, and (3) availability at commercial scale. Several process parameters such as the gap between nozzle and wheel, the angle of incidence of melt, the speed of rotation copper wheel, initial melt temperature, ejection pressure and material properties such as

density, surface tension, viscosity, thermal conductivity influence the quality of as-spun ribbons. Among these parameters, the speed of the wheel is an important parameter in determining the thickness of the ribbon; the faster the wheel rotates, the thinner is the ribbon. For example, a $Fe_{40}Ni_{40}B_{20}$ alloy cast on a 250 mm diameter copper wheel rotating at a substrate velocity of 26.6 ms^{-1} produced a ribbon of 37 µm thickness, while at a velocity of 46.5 ms^{-1}, the ribbon thickness was only 22 µm [11]. However, it is quite challenging to produce ultrathin smooth ribbons thinner than 10 µm by conventional melt spinning. This is due to gas bubbles entrained at the melt-roller interface during casting causing surface roughness and pockets in the ribbons.

In this work, a conventional melt-spinner was used to produce the ultra-thin ribbons. This was achieved by varying the speed of the wheel. At the first stage, the master alloy of Co-Fe-B-Si-Nb was prepared by arc-melting of pure elements Fe (99.9%), Co (99.99%), B (99.5%), Nb (99.9%) and Si (99.9%) in a highly pure argon atmosphere with Titanium as a getter material to reduce the possibility of oxidation. The ingots (20-30 g) were re-melted at least ten times (5 times on each side) to assure a homogeneous composition of ingots. Prior to re-melting, the ingots were broken into several pieces (4-5 g) and were re-melted in quartz tubes by induction heating. After raising the temperature to the liquidus, a dwell of at least 120 seconds was used to ensure that the ingots were completely melted. A quartz tube with an orifice diameter of 0.4 mm was utilised to eject the melt onto the surface of a copper wheel with a diameter of 20 cm which was used to quench the amorphous ribbons. The chamber was evacuated down to $3x10^{-5}$ Torr pressure, and then Argon gas was introduced in the chamber (30 cm Hg) to avoid any possible leaks of the chamber. The gap between the quartz nozzle orifice and the surface of the Cu-wheel was maintained at 0.2 mm by a meter gauge detector. Argon was used as ejection gas, and the ejection pressure (0.1 Kg f/cm) was kept constant during the whole series of experiments. The speed of the Cu-wheel was increased gradually, and its effect on the thickness of the quenched ribbons was investigated. The thickness of the ribbons was measured by a micrometre and finally calibrated by the scanning electron microscopy (SEM) imaging. Thin ribbons of approximately 1 mm width and 10 cm

length were fabricated. Table I summarises the effect of speed of copper wheel on the thickness of the amorphous ribbons.

Table I: Effect of wheel speed on the thickness of the ribbons

Speed of Cu wheel (rpm)	**Thickness of ribbons (μm)**
2530	30
3550	20
4030	15
4470	11.5
4968	8
5100	5.5

A higher rotation speed of the copper wheel enables the fabrication of thinner ribbons and also means that material experiences a higher cooling rate. It is generally accepted that the solidification rate, *R*, is inversely proportional to the square of the thickness of the solidified molten layer. For a layer of thickness '*x*' solidified at a heat transfer coefficient ∞, the solidification rate can be calculated from equation 1.

$$R = \frac{A}{x^2} \quad \text{---------- (1)}$$

Where constant *A* is a function of the material properties and initial temperatures but is independent of *x*. Assuming an estimated value of $A = 10^{-3}$ m^2 Ks^{-1}, the solidification rate achieved will be approximately 10^5 Ks^{-1} for $x = 100$ μm and 10^9 Ks^{-1} for $x = 1$ μm [11]. Based on this relation, the cooling rates experienced by the ribbons as a function of their thickness were calculated and presented in Fig 1.

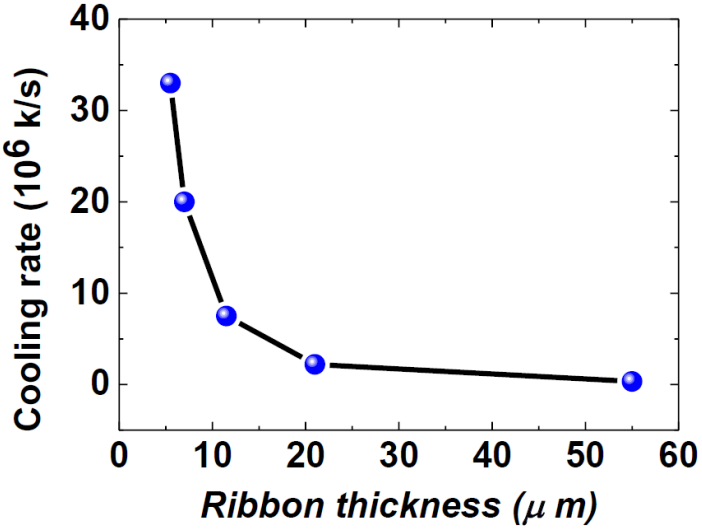

Fig. 1. Estimated cooling rates experienced by ribbons of different thickness.

3. RESULTS AND DISCUSSION

3.1. Atomic structure and surface morphology of ribbons

Fig. 2 presents the structural analysis of the as-quenched amorphous ribbons by X-ray diffraction (Cu-Kα radiation, λ=1.54 Å, Siemens 5000) and magneto-thermogravimetric (MTG) technique. The XRD spectrum of ultra-thin (5.5 µm) and 20 µm as-quenched ribbons showed similar diffraction patterns with a broad maxima in the range of 2θ=40-50^o (Fig. 2a). The presence of a broad hallow and the absence of Bragg's peaks in the diffraction patterns confirm the disordered atomic structure of the ribbons. Additionally, the Curie temperature (T_c) depends on the state of the atomic structure and could be useful to trace a minimal phase precipitated during the rapid quenching process [8]. The temperature dependent magnetisation [*M (T)*] of 5.5 µm and 20 µm ribbons are presented in Fig. 2(b). Both samples revealed a single phase *M (T)* behaviour without showing any "kink" before reaching the T_c (i.e.440 ^{o}C). The overlapped M (T) curves of both samples show that the atomic structure of ribbons was monolithic amorphous until crystallisation at 510 ^{o}C.

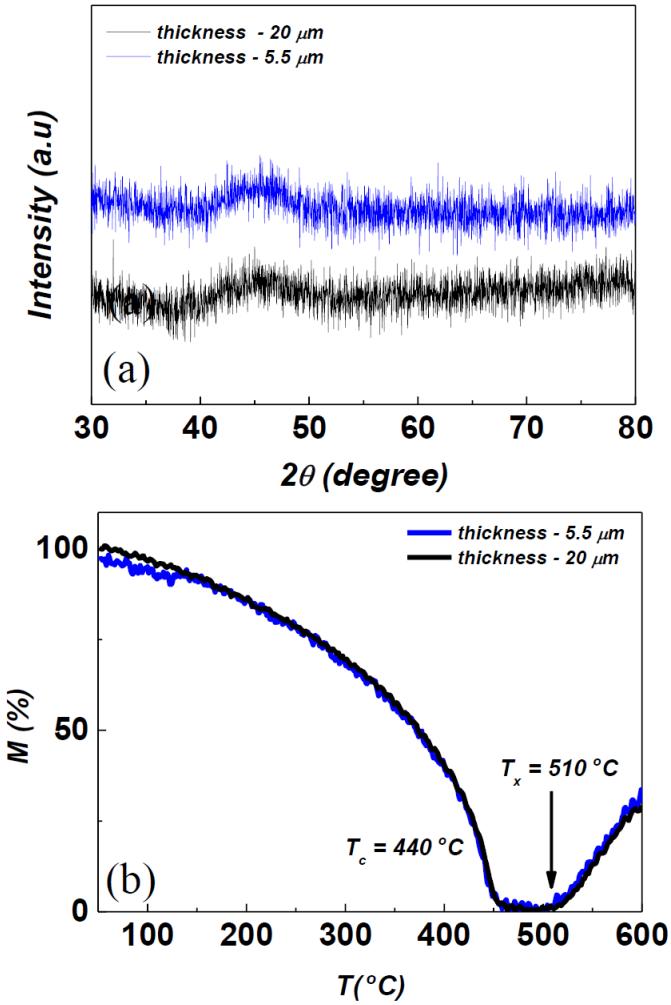

Fig. 2. (a) The x-ray diffraction (XRD) patterns of 5.5 µm and 20 µm ribbons, (b) The temperature dependent magnetic behaviours, *M (T)*, of 5.5 µm and 20 µm ribbons were measured by using a magneto-thermogravimetric technique.

The surface morphology of ribbons was investigated using scanning electron microscopy (SEM) and a profilometer as presented in Fig. 3. The cross-sectional image of the thinnest ribbon is presented in Fig. 3 (a). The SEM micrographs of the surface of the ribbons show that surface of amorphous ribbons becomes dramatically rough when the thickness reduced to 5.5 µm. In addition, the roughness of amorphous ribbons was evaluated by a profilometer and presented in Fig. 3 (f). The roughness of thinner ribbons is significantly high and in agreement with the SEM observations. Despite the very rough surface, the ultra-thin ribbons were continuous without any pores over a large scale.

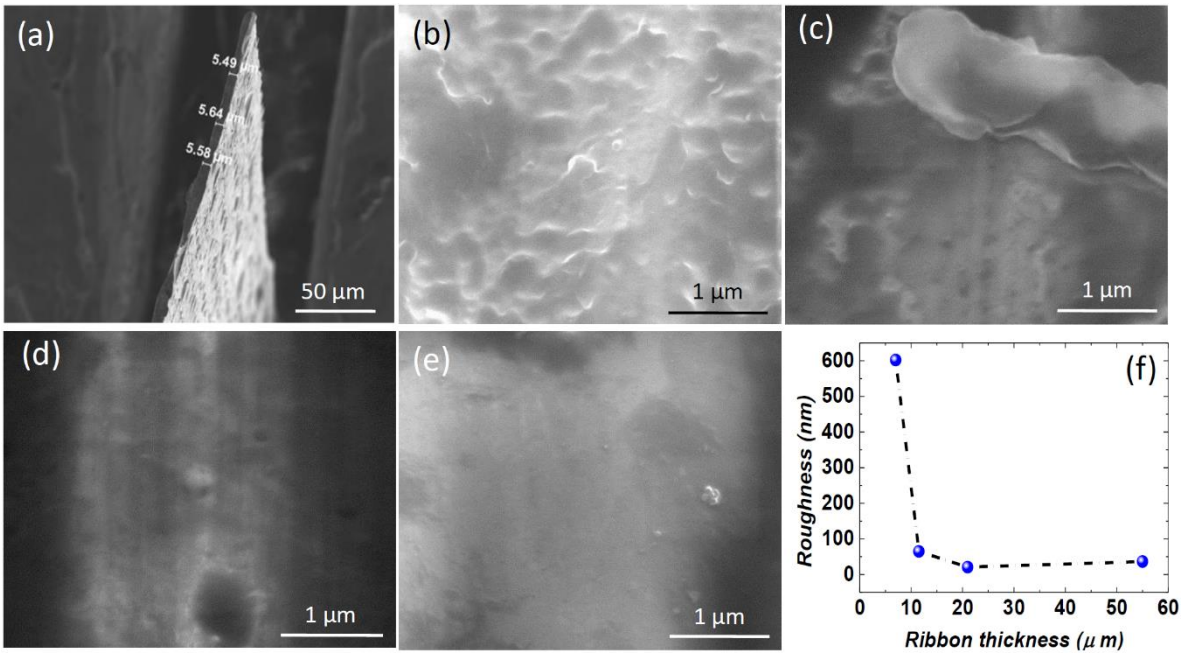

Fig. 3: (a) SEM micrograph of the cross-section of the thinnest ribbon. SEM micrographs of the surface of ribbons: (b) 5.5 µm, (c) 7 µm, (d) 11.5 µm, (e) 21 µm. (f) the surface roughness of the ribbons measured by a profilometer.

3.2. Magnetic properties of amorphous ribbons

Fig. 4 represents the quasistatic soft magnetic properties of the as-quenched amorphous ribbons. The in-plane magnetic hysteresis loops, illustrated in Fig. 4(a), were carried out by a BH-loop tracer (SHB, MESA 200HF) along the length (25 mm) of the ribbons by applying a maximum field of 40 kA/m and were utilised to measure the coercivity (H_c) of the samples. Fig. 4 (b) presents the thickness dependent H_c of amorphous ribbons, while the inset illustrates the magnetic response of the material at low magnetic fields. Ultra-low $H_c < 0.5$ A/m of amorphous ribbons (≥ 21 µm) show the radical soft magnetic behaviour of the alloy. The exceptional soft magnetic properties of as-quenched ribbons confirmed that magnetoelastic contribution to magnetic properties was negligible and magnetostriction constant of the amorphous alloy is close to zero. Nevertheless, the H_c gradually increased as a function of thickness and reached to 5 A/m for 5.5 µm ultra-thin ribbons.

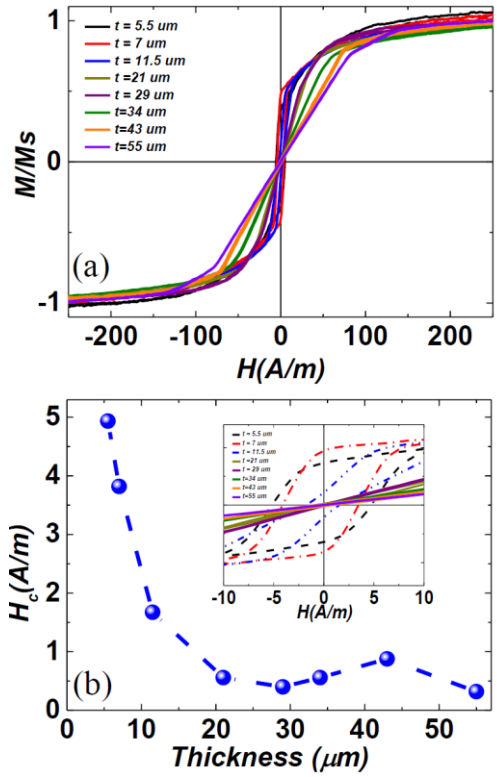

Fig. 4. (a) Hysteresis loops of the samples with different thicknesses, (b) coercivity of the amorphous ribbons as a function of their thicknesses.

The thickness dependent soft magnetic behaviour of amorphous ribbons can largely be explained by the contribution of surface inhomogeneities produced during the quenching process. The relatively high value of H_c is likely due to pinning of the domain walls at the large surface irregularities observed (Fig. 3) in thinner ribbons. In such a case, when magnetisation reversal process is dominated by the pinning of the domain walls due to thickness dependent roughness, the H_c is inversely related to the thickness of the sample as shown in *eq*. 2.

$$H_C \propto \frac{\gamma}{t} \quad \text{---------- (2)}$$

Where t is the ribbon thickness, and γ is the domain wall energy [12]. In a multidomain regime, the magnetisation reversal process is due to the domain wall motion, and the domain wall propagates in an energy landscape influenced by some of the factors, such as grain boundaries, surface roughness, and defects. Therefore, the potential barriers and potential

minima, the so-called pinning sites, inhibit the nucleation and propagation of the domain walls. Thus, in thinner ribbons surface irregularities act as local barriers, which may inhibit the nucleation and motion of the domain wall, during the magnetisation reversal. The H_c, which is required to overcome these barriers, was seen to increase with the decreasing ribbon thickness (see Fig. 4 b). The contribution to H_c should be rather low for bulk cast ($\geq$ 20 μm) samples because (i) the surface upon casting is very smooth and (ii) the thickness is significantly larger than the ultra-thin ribbons resulting in a higher proportion of volume to surface area in thicker ribbons.

In addition to the surface inhomogeneities, the partial instability of free volume below melting point in the disorder atomic structure, known as voids, are the source of pinning sites for the domain wall motion[13, 14]. The voids in amorphous metals are similar to the defects in crystalline materials and work as stress sources [14]. The possibility of originating voids is much higher at extremely high cooling rates due to an immediately frozen liquid state of the alloy, hence leads to a high level of stored internal stress in thinner ribbons. The fluctuation of internal stress or the number of voids can be reduced by annealing the amorphous alloys in the supercooled regime before crystallisation [7]. The 5.5 μm amorphous ribbons were annealed at 480 ^{o}C for 600 sec and characterised for their soft magnetic properties. The coercivity (H_c=1.6 A/m) of the ribbons was reduced by a factor of three after annealing. The improved soft magnetic properties could be attributed to the highly dense disorder atomic structure, and a reduced number of voids attained during the annealing process [7].

4. CONCLUSIONS

A rapid quenching approach of in-situ thinning was developed to produce ultra-thin amorphous ribbons of Co-Fe-B-Si-Nb alloy. The ultra-thin amorphous ribbons were continuous without any pores over a large scale and retain excellent soft magnetic properties. The thickness dependent magnetic properties of the amorphous ribbons were largly attributed to the surface inhomogenities and voids produced during the quenching process.

The in-situ thinning process of amorphous ribbons significantly reduces the cost of amorphous ribbons by consuming less amount of material. In addition, it eliminates the need for post-processing steps to reduce the thickness of ribbons to get an advantage of reduced eddy currents at high frequencies. The in-situ thinning process of amorphous alloys improves materials' performance, reduced material's cost and provides the opportunity for mass production of the high flux density soft magnetic amorphous materials at relatively lower costs.

Acknowledgements

The authors would like to thank CCAN and Enterprise Ireland (EI) for the financial support to perform the research work. Authors would like to thank Nuvotem Talema, Energy Limited, Excelsys Technologies for supporting the research program.

References:

1. Kulkarni, S., et al., *Low Loss Magnetic Thin Films for Off-Line Power Conversion.* Ieee Transactions on Magnetics, 2014. **50**(4).
2. Masood, A., et al., *Controlling the competing magnetic anisotropy energies in FineMET amorphous thin films with ultra-soft magnetic properties.* Aip Advances, 2017. **7**(5).
3. Masood, A., et al., *Tailoring the ultra-soft magnetic properties of sputtered FineMET thin films for high-frequency power applications.* 8th Joint European Magnetic Symposia (Jems2016), 2017. **903**.
4. Kulkarni, S., et al., *Low loss thin film magnetics for high frequency power supplies.* 2014 16th European Conference on Power Electronics and Applications (Epe'14-Ecce Europe), 2014.
5. Masood, A., et al., *The effect of Ni-substitution on physical Properties of Fe72-xB24Nb4Nix Bulk Metallic Glassy Alloys.* MRS Proceedings, 2011. **1300**.
6. Masood, A., et al., *Co-based amorphous thin films on silicon with soft magnetic properties.* Aip Advances, 2018. **8**(5).
7. Masood, A., et al., *Effect of Ni-substitution on glass forming ability, mechanical, and magnetic properties of FeBNbY bulk metallic glasses.* Journal of Applied Physics, 2013. **113**(1).
8. Lee, S., et al., *Magneto-Thermo-Gravimetric technique to investigate the structural and magnetic properties of Fe-B-Nb-Y Bulk Metallic Glass.* 13th International Conference on Rapidly Quenched and Metastable Materials, 2009. **144**.
9. Ackland, K., et al., *Ultra-soft magnetic Co-Fe-B-Si-Nb amorphous alloys for high frequency power applications.* Aip Advances, 2018. **8**(5).
10. Silveyra, J.M., et al., *High performance of low cost soft magnetic materials.* Bulletin of Materials Science, 2011. **34**(7): p. 1407-1413.
11. Suryanarayana, C. and A. Inoue, *Bulk Metallic Glasses.* Bulk Metallic Glasses, 2011: p. 1-523.
12. Kim, Y.M., et al., *Thickness effects on magnetic properties and ferromagnetic resonance in Co-Ni-Fe-N soft magnetic thin films.* Journal of Applied Physics, 2002. **91**(10): p. 8462-8464.

13. Bitoh, T., A. Makino, and A. Inoue, *Origin of low coercivity of Fe-(Al, Ga)-(P, C, B, Si, Ge) bulk glassy alloys.* Materials Transactions, 2003. **44**(10): p. 2020-2024.
14. Bitoh, T., A. Makino, and A. Inoue, *Quasi-dislocation dipole-type defects and low coercivity of Fe-based soft magnetic glassy alloys.* Metastable, Mechanically Alloyed and Nanocrystalline Materials, 2005. **24-25**: p. 427-430.